International Journal of Pharmaceutics 548 (2018) 159–172

Contents lists available at ScienceDirect

International Journal of Pharmaceutics

journal homepage: www.elsevier.com/locate/ijpharm

Formulation of delivery systems with risperidone based on biodegradable terpolymers

Artur Turek[a,*], Aleksandra Borecka[b], Henryk Janeczek[b], Michał Sobota[b], Janusz Kasperczyk[a,b]

[a] School of Pharmacy with the Division of Laboratory Medicine in Sosnowiec, Medical University of Silesia, Katowice, Chair and Department of Biopharmacy, Jedności 8, 41-200 Sosnowiec, Poland

[b] Centre of Polymer and Carbon Materials, Polish Academy of Sciences, M. Curie-Skłodowskiej 34, 41-819 Zabrze, Poland

ARTICLE INFO

Keywords:
Risperidone
Terpolymers
Solution casting
Hot melt extrusion
Formulation

ABSTRACT

Risperidone is applied in oral dosage formulations in the treatment of mental diseases. Current trends point toward parenteral delivery systems based on poly(lactide-co-glycolide), with wafers or rods being the more attractive option than the routinely used intramuscular suspension with microparticles. The aim of our work was to study the utility of solution casting and hot melt extrusion in the formulation of wafers and rods with risperidone based on terpolymers, namely poly(lactide-co-glycolide-co-trimethylene carbonate) and poly(lactide-co-glycolide-co-ε-caprolactone). Synthesis of the terpolymers was carried out by using a non-toxic zirconium initiator and a racemic (LL/DD) or optically active form of the lactide monomer. The delivery systems were analyzed by NMR, DSC, GPC, and SEM. The release profile was monitored by HPLC. Terpolymer chain microstructure, glass transition temperature, and morphology revealed unchanged values after formulation. Solution casting resulted in a drop in molecular weight to a smaller degree than hot melt extrusion. The presence of risperidone influenced another decrease in molecular weight. Both methods are adequate for the formulation of delivery systems based on terpolymers for prolonged release of risperidone. An adequate selection of monomer composition in terpolymers allows to control the release period. Risperidone was released in three phases, however, the burst effect was observed for poly(L-lactide-co-glycolide-co-ε-caprolactone).

1. Introduction

Risperidone (RSP) is administered via solutions, oral tablets, and orally disintegrating tablets in the treatment of mental diseases. However, current trends point toward the development of parenteral formulations which are characterized by prolonged release. Only one medicinal product with long-acting RSP has been available on the market in the form of intramuscular poly(D,L-lactide-co-glycolide) (D,L-PLGA) 75:25 microparticles that are obtained by the encapsulation method and administered as an aqueous suspension (EMEA, 2017; Harrison and Goa, 2004). Other microparticles are also being developed and optimized based on the other copolymers of lactide (LA) and glycolide (GA) with various contents of comonomeric units, i.e., mainly in the range of 50:50–85:15, and with a different configuration of LA (Acharya et al., 2010; An et al., 2016; D'Souza et al., 2014a,b; Hu et al., 2011; Jafarifar et al., 2016; Selmin et al., 2012; Shen et al., 2016; Song et al., 2014; Su et al., 2009; Tian et al., 2014; Wang et al., 2002). The latest data in the literature show that PLGA microparticles may ensure prolonged release of RSP, i.e., between 20 and 50 days (Acharya et al., 2010; D'Souza et al., 2013, 2014a; Lu et al., 2014; Selmin et al., 2012; Shen et al., 2015; Su et al., 2009). Yet they are administered as an aqueous suspension, which may cause pain (Fleischhacker et al., 2003; Martin et al., 2003). The microparticles may generate a significant burst effect because of their surface size, according to the general rule that the smaller the particles are, the faster the release will be. Moreover, the microparticles cannot be removed if any side effects appear.

Solid formulations such as wafers and rods that can be administered cutaneously, subcutaneously, or intramuscularly are a more attractive

Abbreviations: CL, ε-caprolactone; *Đ*, Molecular weight distribution; D,L-PLGA, racemic poly(D,L-lactide-co-glycolide); DSC, differential scanning calorimetry; F_{CL}, molar percentage of caproyl units; F_{GG}, molar percentage of glycolidyl units; F_{LL}, molar percentage of lactidyl units; F_{TMC}, molar percentage of carbonate units; GA, glycolide; GPC, gel permeation chromatography; HME, hot melt extrusion; LA, lactide; l_{CL}, average length of caproyl blocks; l_{GG}, average length of glycolidyl blocks; l_{LL}, average length of lactidyl blocks; l_{TMC}, average length of carbonate blocks; M_n, molecular weight; NMR, nuclear magnetic resonance; P(D,L-LA:GA:CL), racemic poly(D,L-lactide-co-glycolide-co-ε-caprolactone); P(D,L-LA:GA:TMC), racemic poly(D,L-lactide-co-glycolide-co-trimethylene carbonate); P(L-LA:GA:CL), optically active poly(L-lactide-co-glycolide-co-ε-caprolactone); P(L-LA:GA:TMC), optically active poly(L-lactide-co-glycolide-co-trimethylene carbonate); RSP, risperidone; SC, solution casting; SEM, scanning electron microscope; T_c, crystallization temperature; T_g, glass transition temperature; T_m, melting temperature; TMC, trimethylene carbonate; T_r, temperature of structural relaxation; $Zr(Acac)_4$, zirconium (IV) acetylacetonate

* Corresponding author.
E-mail address: artur.turek@sum.edu.pl (A. Turek).

https://doi.org/10.1016/j.ijpharm.2018.06.051
Received 19 February 2018; Received in revised form 21 June 2018; Accepted 22 June 2018
Available online 25 June 2018
0378-5173/

option than intramuscular suspensions with microparticles because of the special precautions that need to be taken on a step-by-step basis when they are handled in order to ensure successful administration (EMEA, 2017). Wafers and rods additionally allow for invasiveness reduction and removal in case there are any side effects. Also, a greater amount of drug substance can be introduced into wafers and rods, which ensures longer action.

Three aspects are significantly important in the design of pharmaceutical formulations. These are: (i) features of the drug substance, (ii) features of the drug carrier, and (iii) the obtaining process. Generally, RSP is well known as a drug substance, and its mechanisms of action and pharmacodynamics (Janssen et al., 1988; Megens et al., 1988), side effects (Borison et al., 1992; Hillert et al., 1992), and both physical and chemical properties (An et al., 2016; Weng et al., 2016) are known. Therefore, RSP is an adequate substance for developing drug delivery systems for prolonged action.

Further development of a drug delivery system for RSP also involves the use of novel materials. In this study, terpolymers based on LA with different configurations, GA, trimethylene carbonate (TMC), or ε-caprolactone (CL) were applied. These materials' mechanical properties were the subject of a previous study. The tests showed that scaffolds based on pointed terpolymers for the treatment of large bone defects using a minimally invasive surgery approach preserved optimal mechanical properties (Rychter et al., 2015). It was also shown that the presence of a drug substance (e.g., sirolimus 7%-wt) had no influence on the mechanical properties (Jaworska et al., 2015).

The terpolymers applied above allowed to modify and prolong the release profile in comparison to routinely used PLGA copolymers which degrade in bulk. Conversely, poly(TMC) undergoes surface erosion (Turek et al., 2016), and commercial long-acting RSP based on D,L-PLGA 75:25 releases the drug substance for only 7–8 weeks (EMEA, 2017).

In mental disease, treatment lasts a lifetime; therefore aspects of the biocompatibility and biodegradability of polymer drug carriers are significantly important. In this study, terpolymers were synthesized using a low-toxic initiator of polymerization, namely zirconium (IV) acetylacetonate ($Zr(Acac)_4$), which ensured lower tissue irritation in comparison to commercially available polymers obtained using stannous compounds as initiators. This aspect of the proposed terpolymers was also described previously (Czajkowska et al., 2005; Orchel et al., 2013; Rychter et al., 2015; Zini et al., 2007).

Another important issue in pharmaceutical manufacture is optimizing the formulation conditions, and various methods can be used to obtain drug delivery systems. The formulation process should not significantly influence the properties of either the drug substance or the polymer carrier. Encapsulation is used as a formulation method for commercial medicinal products with microparticles containing RSP, although this method requires large amounts of the solvent. There is also often an aqueous solution that may change the properties of the drug substances and the aliphatic polyesters and polycarbonates (Chen et al., 2014; Fredenberg et al., 2011; Selmin et al., 2012). Solid pharmaceutical formulations such as wafers and rods obtained by solution casting (SC) and hot melt extrusion (HME) may either decrease or eliminate the solvents, and they are currently the most often applied methods (Cicero and Dorgan, 2001; Gogolewski et al., 1993; Jelonek et al., 2011; Kasperczyk et al., 2009; Li et al., 2013a,b; Ma and McHugh, 2010; Manson and Dixon, 2012; Nuutinen et al., 2002; Rattanakit et al., 2012; Ro et al., 2012; Rothen-Weinhold et al., 1997, 1999; Simpson et al., 2015; Turek et al., 2010, 2013, 2015, 2016; Yen et al., 2009; Yuan et al., 2001). SC is often used in preliminary studies for its simplicity, low cost, and possibility of avoiding thermal degradation (Jelonek et al., 2011; Kasperczyk et al., 2009; Turek et al., 2015). It constitutes an interesting method due to processing at room temperature, and thus may be of interest particularly with temperature-sensitive compounds. However, slow solvent removal and hardening of the formulations may be associated with separation of the drug substance and the polymer (Wischke and Schwendeman, 2012), drug substance sedimentation, or plastification caused by the presence of solvent residues (Santoveña et al., 2005; Snejdrova et al., 2015; Snejdrova et al., 2016). In turn, HME allows to precisely control the shape and size of the implants but increases the risk of overheating and thermal degradation (Cicero and Dorgan, 2001; Ellä et al., 2011; Gogolewski et al., 1993; Liu et al., 2006; Nuutinen et al., 2002; Rothen-Weinhold et al., 1997; Rothen-Weinhold et al., 1999; Simpson et al., 2015; Yen et al., 2009; Yuan et al., 2001).

The aim of our work was to study the utility of SC and HME in the formulation of wafers and rods with RSP based on racemic poly(D,L-lactide-co-glycolide-co-trimethylene carbonate) (P(D,L-LA:GA:TMC)), optically active poly(L-lactide-co-glycolide-co-trimethylene carbonate) (P(L-LA:GA:TMC)), racemic poly(D,L-lactide-co-glycolide-co-ε-caprolactone) (P(D,L-LA:GA:CL)), and optically active poly(L-lactide-co-glycolide-co-ε-caprolactone) (P(L-LA:GA:CL)) synthesized with a low-toxic initiator via: (i) synthesis of the terpolymers, (ii) determining the thermal properties of RSP and raw terpolymers in order to optimize the conditions of the formulations (wafer and rod), (iii) conducting a study of the composition, chain microstructure, and molecular weight (M_n) of raw terpolymers, (iv) release profiles, and (v) the influence of SC and HME on the composition and chain microstructure, thermal parameters, molecular weight, and morphological features of the formulations.

2. Materials and methods

2.1. Terpolymers

P(D,L-LA:GA:TMC), P(L-LA:GA:TMC), P(D,L-LA:GA:CL), and P(L-LA:GA:CL) were synthesized at the Centre of Polymer and Carbon Materials of the Polish Academy of Sciences in Zabrze in bulk using $Zr(Acac)_4$ as a low-toxic initiator according to a previous methodology (Dobrzynski et al., 2013). Synthesis of the terpolymers was carried out using a reactor from the Parr Instrument Company (4550 Floor Stand Pressure Reactor) with computer control of the polymerization parameters. The polymerization process was conducted in a melt at 120 °C for 72 h. The materials were purified by dissolution in chloroform and adding dropwise to cold methanol. Then the terpolymers were dried under vacuum conditions at 25 °C. All of the monomers that were used, except for CL, were purified by recrystallization from ethyl acetate, dried in air conditions and then dried in a vacuum oven at room temperature. CL was dried and purified by distillation over calcium hydride.

2.2. Solution casting

Blank wafers (wafers) 9.9 mm ± 0.011 mm in diameter and 0.3 mm ± 0.023 mm thick and wafers with RSP (wafers-RSP) (10%-wt, Teva, Kutno, PL) 10.0 mm ± 0.012 mm in diameter and 0.3 mm ± 0.023 mm thick were formulated by SC at 25 °C.

Before the process, raw terpolymers were dried under air conditions in a laminar box for 7 days. The dry terpolymers were subjected to grinding at a temperature of -196 °C in a cryogenic mill (6870 SPEX, USA) and dried again with the use of a drying set containing a dryer (Memmert VO500) and a pump (BUCHI V-710) for 14 days in a temperature of 23 °C and at a pressure of 80 mbar.

A total of 1.0 g of terpolymers in 1.5 mL of methylene chloride (POCH, Gliwice, PL) was used for the wafer formulations, whereas RSP and the terpolymers were dissolved in methylene chloride (POCH, Gliwice, PL) in the following proportions: 0.1 g of RSP in 0.5 mL of solvent and 1.0 g of terpolymer in 1.5 mL of solvent for wafers-RSP. The obtained mixtures were deprived of air under a vacuum line, cast on Teflon molds and left for solvent evaporation in a laminar box (7 days)

followed by drying under a vacuum (7 days).

2.3. Hot melt extrusion

Blank rods (rods) 1.0 mm ± 0.014 mm in diameter and 1.0 mm ± 0.007 mm long and rods with RSP (rods-RSP) (10%-wt, Teva, Kutno, PL) 1.0 mm ± 0.014 mm in diameter and 1.0 mm ± 0.007 mm long were prepared by HME. Before the process, raw terpolymers were subjected to the same procedure as terpolymers in the SC method. A drug substance was introduced to the milled dry terpolymers and thoroughly mixed by vortex for 10 min.

Terpolymers or mixtures of terpolymers and RSP were fed into an extruder cylinder heated to 105 °C. The extrusion process was carried out in a co-rotating twin screw extruder (Minilab, Thermo-Haake, GE) using a plasticizing screw at a rotational speed of 20 rpm. The plasticized material was pressed through a die 0.7 mm in diameter and received on cooled rolling devices. The formulated rod, 1 mm in diameter, was cut into 1 cm pieces.

2.4. Terpolymer composition and chain microstructure study

The composition and chain microstructure of the raw terpolymers, wafers, wafers-RSP, rods, and rods-RSP were analyzed by nuclear magnetic resonance spectroscopy (NMR). Spectra were recorded using a Bruker-Avance II Ultrashield Plus spectrometer operating at 600 MHz (^{1}H) and 150 MHz (^{13}C) using DMSO-d_6 as a solvent with a 5.0 mm sample tube. ^{1}H NMR spectra were obtained with 32 scans, 11 μs pulse width, and 2.65 s acquisition time; ^{13}C NMR spectra were obtained with 20 000 scans, 9.4 μs pulse width, and 0.9 s acquisition time. The analyses were performed in 80 °C. Signals observed in ^{1}H and ^{13}C NMR spectra were assigned to appropriate sequences in the terpolymer chain, and parameters such as molar percentage of lactidyl units (F_{LL}), glycolidyl units (F_{GG}), carbonate units (F_{TMC}), caproyl units (F_{CL}), average length of lactidyl blocks (l_{LL}), glycolidyl blocks (l_{GG}), carbonate blocks (l_{TMC}), and caproyl blocks (l_{CL}) were calculated according to a previously described procedure (Gebarowska et al., 2011) and based on the following, newly developed equations (Table 1, Eqs. (1)–(4); Table 2, Eqs. (5)–(8)).

2.5. Thermal study

The thermal characteristics of RSP, raw terpolymers, wafers, wafers-RSP, rods, and rods-RSP were analyzed by means of differential scanning calorimetry (DSC) using a TA DSC 2010 apparatus (TA Instruments, New Castle, DE) in a range from -30 °C to 220 °C under nitrogen atmosphere (flow rate = 50 mL/min). The instrument was calibrated with high purity indium. Two heating runs were performed for all samples. The first run for the initial samples and the second run for the amorphous samples were obtained by quenching from a melt (220 °C). The values of the melting temperature (T_m), glass transition temperature (T_g), and crystallization temperature (T_c) were determined.

Table 1
Equations for F_{LL}, F_{GG}, F_{TMC}, and F_{CL} calculations based on ^{1}H NMR spectra.

F_{LL}	$F_{LL} = \frac{2n_{LL}}{n_{LL} + n_{GG} + 1}$	Eq. (1)
F_{GG}	$F_{GG} = \frac{2n_{GG}}{n_{LL} + n_{GG} + 1}$	Eq. (2)
F_{TMC}	$F_{TMC} = \frac{2n_T}{n_{LL} + n_{GG} + 1}$	Eq. (3)
F_{CL}	$F_{CL} = \frac{n_C}{n_{LL} + n_{GG} + 1}$	Eq. (4)

F_{LL} – molar percentage of lactidyl units in terpolymer.
F_{GG} – molar percentage of glycolidyl units in terpolymer.
F_{TMC} – molar percentage of carbonate units in terpolymer.
F_{CL} – molar percentage of caproyl units in terpolymer.
n – unit contribution.

Table 2
Equations for l_{LL}, l_{GG}, l_{TMC}, and l_{CL} calculations based on ^{13}C NMR spectra.

l_{LL}	$l_{LL} = \frac{0.5(LLL + LLX + XLL + XLX}{XLX + 0.5(LLX + XLL)}$	Eq. (5)
l_{GG}	$l_{GG} = \frac{0.5(GGG + GGY + YGG + YGY}{YGY + 0.5(GGY + YGG)}$	Eq. (6)
l_{TMC}	$l_{TCM} = \frac{TT + ZT}{ZT}$	Eq. (7)
L_{CL}	$l_{CL} = \frac{CC + ZC}{ZC}$	Eq. (8)

l_{LL} – average length of lactidyl blocks.
l_{GG} – average length of glycolidyl blocks.
l_{TMC} – average length of carbonate blocks.
l_{CL} – average length of caproyl blocks.
X – GG or *T* or *C*, *Y – LL* or *T* or *C* and *Z – GG* or *LL*.

The heating rate for pure RSP was 10 °C/min and 20 °C/min for the terpolymer samples. T_g was taken as the midpoint of the heat capacity change for amorphous samples obtained by quenching from a melt (220 °C) in liquid nitrogen.

2.6. Molecular weight study

M_n and molecular weight distribution (D) of the raw terpolymers, wafers, wafers-RSP, rods, and rods-RSP were analyzed by gel permeation chromatography (GPC) with a Physics SP 8800 chromatograph. Tetrahydrofuran was used as the eluent with a flow rate of 1 mL/min, using Styragel columns and a Shodex SE 61 detector. M_n was calibrated with polystyrene standards.

2.7. Morphology study

Electron micrographs of the wafers, wafers-RSP, rods, and rods-RSP were obtained using a Quanta 250 FEG scanning electron microscope (SEM) (FEI Company, USA) operating at an acceleration voltage of 5 kV under low vacuum conditions (80 Pa) from secondary electrons collected by a Large Field Detector (LFD). The samples were glued to microscopic stubs with double-sided adhesive carbon tape.

2.8. RSP release study

The concentration of RSP released from the wafers (n = 10) and rods (n = 10) was determined by high-performance liquid chromatography (HPLC) using an Elite LaChrom HPLC system (VWR Hitachi, Merck) with a UV absorbance detector (Diode Array Detector L-2355, VWR Hitachi, Merck) set at 280 nm. The samples were first purified on filters (ISO Disc Filters pTFE-13–2) sized 13 nm x 0.2 μm (SUPELCO). Separation was performed using a precolumn (LiChroCART 4–4, LiChrospher 60 RP – select B) and columns 5 μm in diameter (LiChroCART 250–4 and LiChrospher RP -18) working in reverse phase. The mobile phase consisted of methanol and ammonium acetate in a ratio of 90:10 and a flow rate of 1 mL/min. The analysis was carried out at a temperature of 40 °C, during a time period of 10 min.

3. Results

3.1. Thermal characterization of RSP

The DSC curve for pure RSP revealed a sharp melting endotherm at 171.0 °C in the first heating run. The second heating scan for the amorphous sample revealed T_g at 29.5 °C. Further heating of the amorphous sample exhibited the “cold” crystallization effect with T_c at 89.8 °C and two melting endotherms at 158.6 °C and 169.1 °C, respectively (Fig. 1).

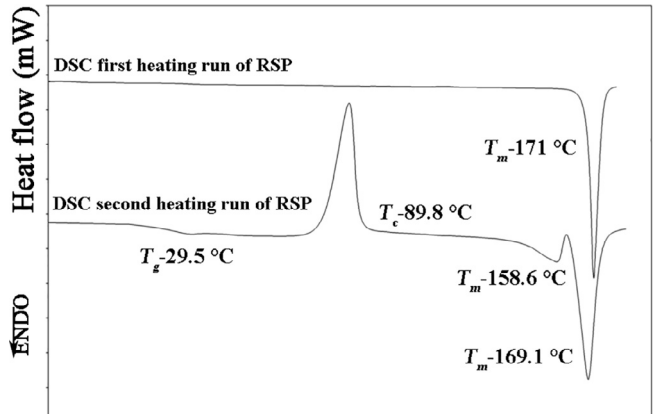

Fig. 1. DSC first heating run of RSP (T_m 171 °C) and DSC second heating run of RSP (T_g 29.5 °C; T_c 89.8 °C; T_m 158.6 °C and T_m −169.1 °C).

3.2. Characterization of raw terpolymers

Terpolymers containing TMC possessed lower F_{LL} (~ 57 mol%) and higher F_{GG} (~ 18 mol%) than terpolymers with CL (~ 70 mol% and ~ 13 mol%, respectively). Differences were also observed in the chain microstructure, as terpolymers with TMC had relatively shorter l_{LL}, l_{GG} and longer l_{TMC} (Figs. 2 and 3, Table 3).

The first DSC heating run revealed no melting endotherms, whereas T_g in the range of 33.8–39.8 °C was determined based on the second heating run (Table 3).

M_n for raw terpolymers showed high values in the range of 49.9–76.3 kDa, and D in the range of 2.015–2.234 (Table 3).

3.3. Characterization of wafers, wafers-RSP, rods, and rods-RSP

3.3.1. Composition and chain microstructure study

Formulations of wafers, wafers-RSP, rods, and rods-RSP based on P(D,L-LA:GA:TMC), P(L-LA:GA:TMC), P(D,L-LA:CL), and P(L-LA:GA:CL) did not result in significant changes of F_{LL}, F_{GG}, F_{TMC}, and F_{CL}, and in l_{LL}, l_{GG}, l_{TMC}, and l_{CL} (Figs. 4–7, Table 4) in comparison to the raw terpolymers (Table 3).

3.3.2. Thermal study

The first heating run of the wafers, wafers-RSP, rods, and rods-RSP did not indicate the presence of melting endotherms. The observed endothermal events resulted from structural relaxation of the rods based on P(L-LA:GA:TMC), P(D,L-LA:GA:CL), and P(L-LA:GA:CL), and rods-RSP based on P(L-LA:GA:CL) (Fig. 8, Table 5). The second heating run indicated that the way of formulation (i.e., SC and HME) and the presence of RPS did not influence the T_g values significantly (Tables 3 and 5).

3.3.3. Molecular weight study

The GPC study for P(D,L-LA:GA:TMC), P(L-LA:GA:TMC), P(D,L-LA:CL), and P(L-LA:GA:CL) wafers revealed that SC resulted in a decrease in M_n (20.04%, 22.79%, 12.32%, and 25.57%, respectively) (Table 5) in comparison to raw terpolymers (Table 3).

M_n values for wafers-RPS revealed an even greater drop after RSP loading (41.48%, 30.10%, 21.49, and 33.97%, respectively) (Table 3) as compared to raw terpolymers (Table 3).

For P(D,L-LA:GA:TMC), P(L-LA:GA:TMC), P(D,L-LA:CL), and P(L-LA:GA:CL) rods, M_n had even lower values after HME (41.68%, 24.15%, 36.96%, and 24.43%, respectively) (Table 5) as compared to raw

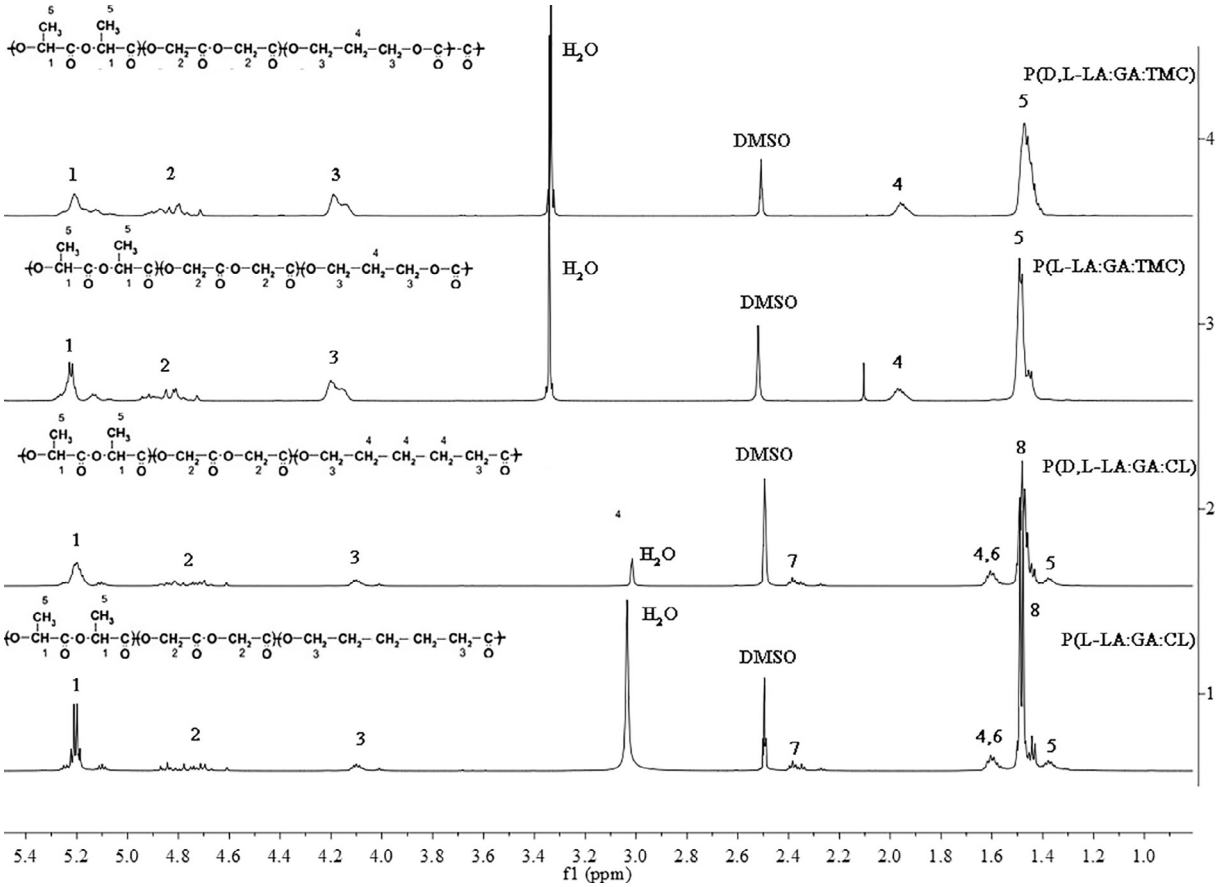

Fig. 2. H^1 NMR spectra of P(D,L-LA:GA:TMC), P(L-LA:GA:TMC), P(D,L-LA:GA:CL), and P(L-LA:GA:CL) raw powders (600 MHz, DMSO-d_6, 80 °C). The methine proton region of lactidyl units and methylene proton region of glycolidyl and carbonate or caproyl units were used for calculations of F_{LL}, F_{GG}, F_{TMC}, and F_{CL}.

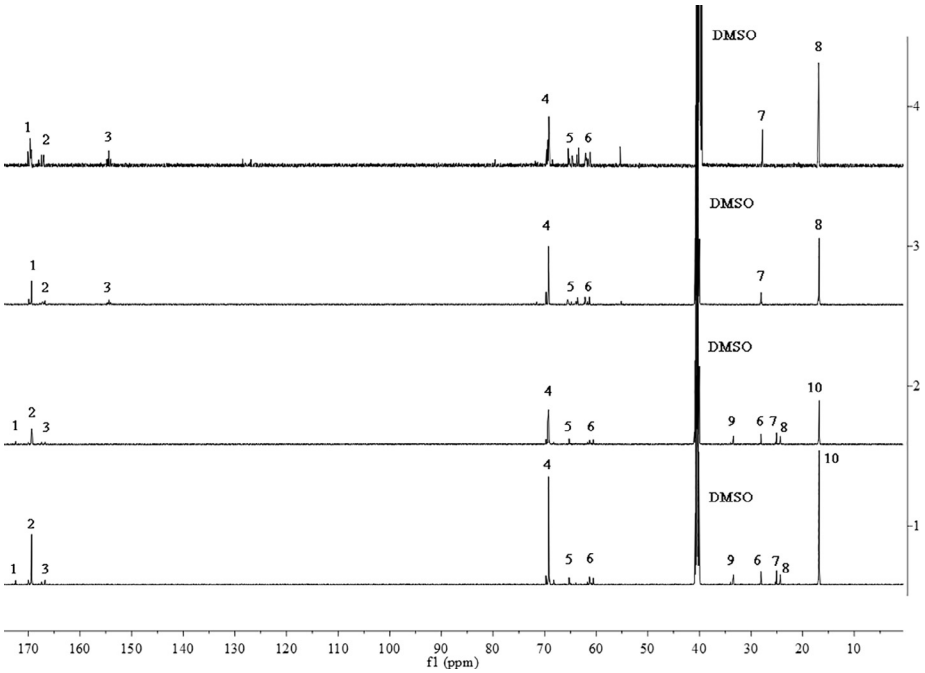

Fig. 3. ^{13}C NMR spectra of P(D,L-LA:GA:TMC), P(L-LA:GA:TMC), P(D,L-LA:GA:CL), and P(L-LA:GA:CL) raw powders (150 MHz, DMSO-d_6, 80 °C). The methine carbon region of lactidyl units (*LL*) and methylene carbon region of glycolidyl (*GG*), carbonate units (*T*), and caproyl units (*C*) were used for calculations of l_{LL}, l_{GG}, l_{TMC}, and l_{CL}.

Table 3
Parameters characterizing raw P(D,L-LA:GA:TMC), P(L-LA:GA:TMC), P(D,L-LA:CL), and P(L-LA:GA:CL).

F_{LL}	F_{GG}	F_{TMC} or F_{CL}	l_{LL}	l_{GG}	l_{TMC} or l_{CL}	T_g	M_n	D
P(D,L-LA:GA:TMC)								
56.6	18.5	24.9	3.9	1.1	1.5	35.0	49.9	2.015
P(L-LA:GA:TMC)								
57.3	18.2	24.5	4.1	1.1	1.5	39.8	58.8	2.108
P(D,L-LA:GA:CL)								
70.5	13.4	16.1	10.3	1.8	1.2	33.8	76.3	2.234
P(L-LA:GA:CL)								
70.3	12.6	17.1	9.2	1.4	1.2	38.2	52.4	2.226

F_{LL} – molar percentage of lactidyl units in terpolymer.
F_{GG} – molar percentage of glycolidyl units in terpolymer.
F_{TMC} – molar percentage of carbonate units in terpolymer.
F_{CL} – molar percentage of caproyl units in terpolymer.
l_{LL} – average length of lactidyl blocks.
l_{GG} – average length of glycolidyl blocks.
l_{TMC} – average length of carbonate blocks.
l_{CL} – average length of caproyl blocks.
T_g – glass transition temperature (°C).
M_n – molecular weight (kDa).
D – molecular weight distribution.

terpolymers (Table 3).

The introduction of a drug substance resulted in a decrease in M_n in a similar manner to wafers (73.35%, 59.69%, 64.87%, and 47.90%, respectively) (Table 5) and when compared to raw terpolymers (Table 3).

3.3.4. Morphology study

The outer morphology of the P(D,L-LA:GA:TMC), P(L-LA:GA:TMC), P(D,L-LA:CL), and P(L-LA:GA:CL) wafers showed a non-porous and monolithic surface. Moreover, no slits and cracks were visible on either sides of the wafers. The introduction of RSP did not result in significant changes in morphology. However, granule-like elements occurred on both the averse and reverse side in some of the wafers. The most significant morphological diversity was observed on the averse side of P(L-LA:GA:CL) wafers-RSP (Fig. 9).

The outer morphology of the P(D,L-LA:GA:TMC), P(L-LA:GA:TMC), P(D,L-LA:CL), and P(L-LA:GA:CL) rods also had a monolithic surface and a lack of perforation, slits, and cracks. Rods made from P(D,L-LA:GA:TMC) and P(D,L-LA:GA:CL) had a more differential topography than the P(L-LA:GA:TMC) and P(L-LA:GA:CL) rods. The inner morphology also revealed a monolithic structure and no pores in the pointed rods. Preparation of the cross-section had an influence on the presence of delamination. Some layers with different areas were visible.

Loading RSP into the rods resulted in changes in morphological features of the surface, i.e., rods made from P(D,L-LA:GA:TMC) and P(D,L-LA:GA:CL) were more diversified than rods made from P(L-LA:GA:TMC) and P(L-LA:GA:CL). The least morphological diversity was observed in P(L-LA:GA:CL) wafers-RSP. A deformation of the P(D,L-LA:GA:CL) rods-RPS was noted. The cross-section also revealed significant delamination because of sample preparation (Fig. 10).

3.3.5. RSP release study

RSP was released in three phases, however, the burst effect was observed in the poly(L-LA:GA:CL) wafers-RSP and rods-RSP. Generally, the release period for the wafers was similar to that for the rods, except for P(L-LA:GA:CL) wafers-RSP, for which it was shorter. Terpolymers with optically active LA revealed a longer release period in comparison to terpolymers with racemic LA (Fig. 11).

4. Discussion

4.1. Thermal properties of RSP

The DSC analysis revealed a crystalline character of RSP in the presence of a melting endotherm at 171 °C (Fig. 1), which was reflected in data in the literature (An et al., 2016; Rahman et al., 2010a; Rahman et al., 2010b). It should be noted that for crystalline substances such as RSP the formulation process should occur below T_m as there is a risk of changes in the substance features.

It should also be noted that tableting and SC require a relatively lower temperature as compared to HME. Based on a thermal analysis of RSP, the temperature conditions for SC at 25 °C and for HME at 105 °C were determined as appropriate, since melting of RSP takes place at 171 °C.

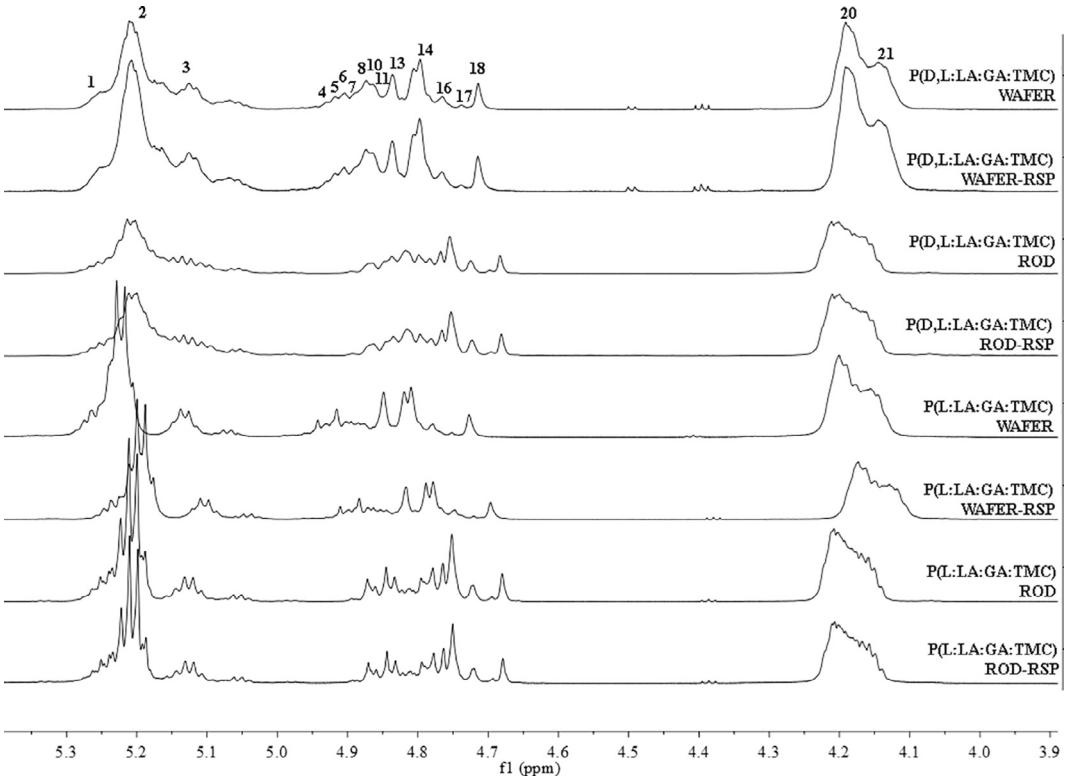

Fig. 4. H^1 NMR spectra of P(D,L-LA:GA:TMC) and P(L-LA:GA:TMC), wafers, wafers-RSP, rods, and rods-RSP (600 MHz, DMSO-d_6, 80 °C). *1-LLG + GLL, 2-LLL, 3-TLL + LLT, 4-GLGGG, 5-GLGGL, 6-GGGGGG, 7-TGGGG + GGGGT + LLGGL + LGGLL, 8-GGGGL + LGGGG, 10-GGGLL, 11-XLGLX (X-T or G), 13-TGGGG, 14-GGGLG, 16-LGGLG, 17-TGGGT, 18-TGGT, 20-LT + GT, 21-TT.*

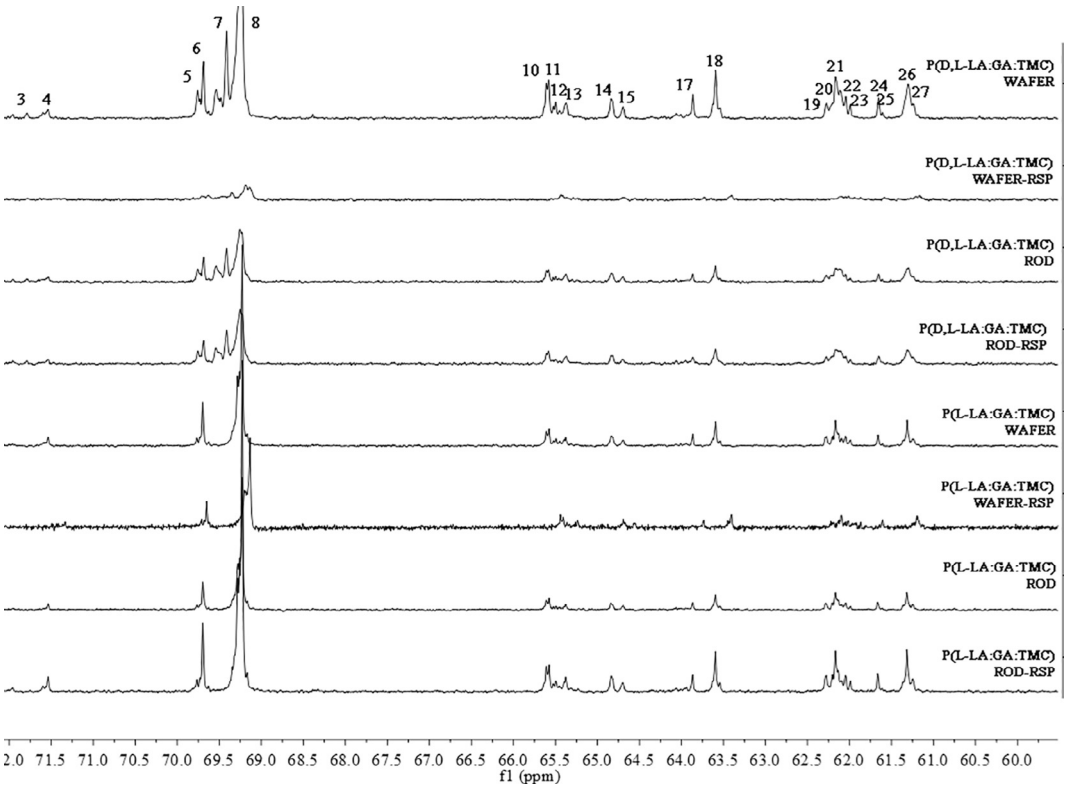

Fig. 5. ^{13}C NMR spectra of P(D,L-LA:GA:TMC) and P(L-LA:GA:TMC), wafers, wafers-RSP, rods, and rods-RSP (150 MHz, DMSO-d_6, 80 °C). *3-TLLLT, 4-TLLLL + TLLLT, 5-GLLT + GLLLT, 6-TLLLL + LLLLT, 7-LLLL, 8-LLGG, 10-TT′G + GGT′GG + TGT′GG, 11-GGTT, 12-GGT′GT + GT′GT, 13-GGT′GT + TT′L + LTT′, 14-TT′T + TTT′ + TT″G, 15-TT′GG, 17-TGT + TGGL + TGGT, 18-LGGGT + TGGGT + GGGGT, 19-TT′L + LT′T, 20-LT′L + LT″L, 21-GGT′T, 22-GGT″GT + GGT″GG, 23-TGT″GG + TGT′GT, 24-TGGGG + TTGG, 25-TGGT, 26-GGLL, 27-GGGG.*

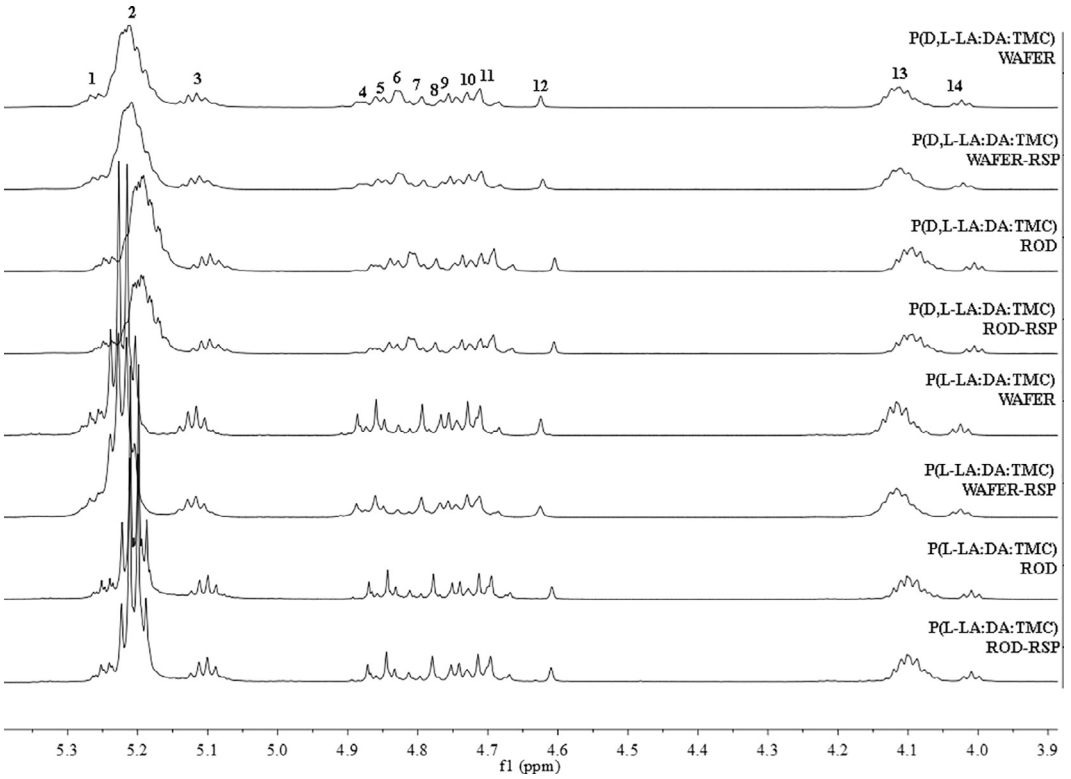

Fig. 6. H^1 NMR spectra of P(D,L-LA:GA:CL) and P(L-LA:GA:CL), wafers, wafers-RSP, rods, and rods-RSP (600 MHz, DMSO-d_6, 80 °C). *1-LLLL, 2-LLGG + LLC + CLL + GGLL, 3-CLC + GLG, 4-GGGG, 5-CGGGG + GGGGC, 6-GGL + LGG, 7-CGGGC, 8-LGL, 9-GGGC, 10-CGGGG + CGGGC, 11-CGGC, 12-CGC, 13-GC + LC, 14-CC.*

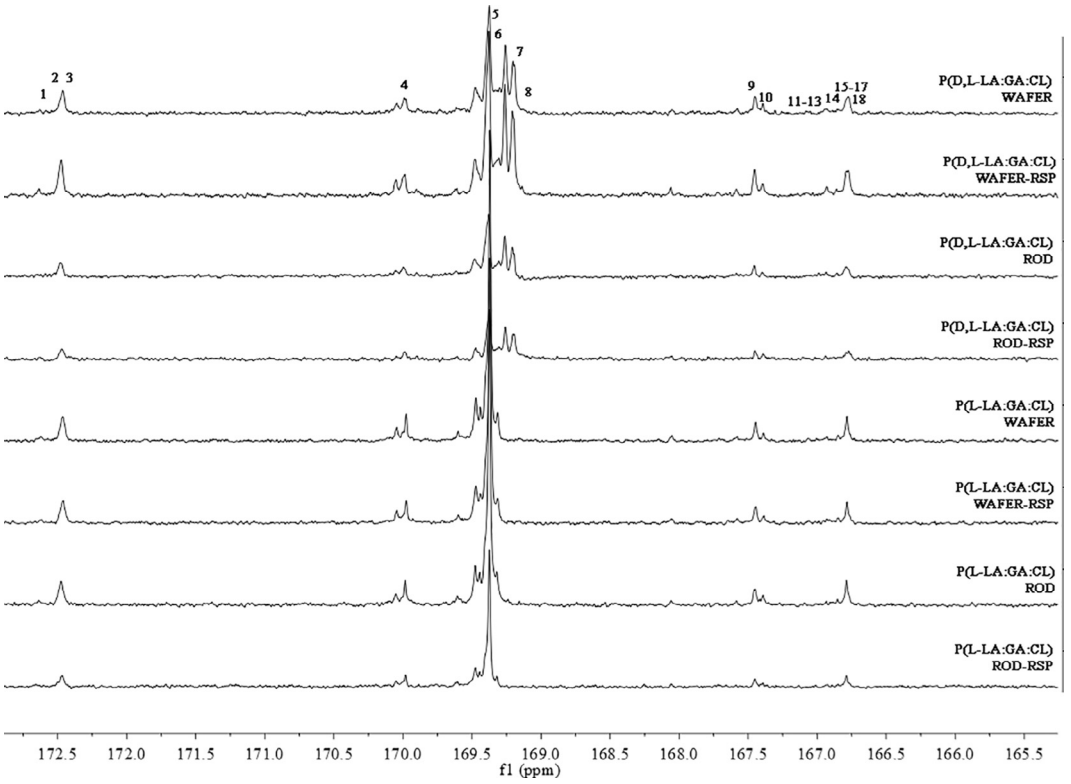

Fig. 7. ^{13}C NMR spectra of P(D,L-LA:GA:CL) and P(L-LA:GA:CL), wafers, wafers-RSP, rods, and rods-RSP (150 MHz, DMSO-d_6, 80 °C). *1-CCC + CGCC + GGCC, 2-CGCGC + GGCGC + LCC + CCL, 3-GGCGG + CCGG + LCL, 4-CLC, 5-CLL + LLC, 6-LLGG, 7-LLLL, 8-GLG, 9-CGC, 10-CGGC, 11-CGGGG, 12-CGGGC, 13-GGGGC, 14-CGGGC, 15-CGGGG, 16-GGGGC, 17-GGGGG, 18-GGLL.*

Table 4
NMR parameters characterizing wafers, wafers-RSP, rods and rods-RSP formulated from P(D,L-LA:GA:TMC), P(L-LA:GA:TMC), P(D,L-LA:CL), and P(L-LA:GA:CL).

Sample	F_{LL}	F_{GG}	F_{TMC} or F_{CL}	l_{LL}	l_{GG}	l_{TMC} or l_{CL}	Sample	F_{LL}	F_{GG}	F_{TMC} or F_{CL}	l_{LL}	l_{GG}	l_{TMC} or l_{CL}
			P(D,L-LA:GA:TMC)							P(L-LA:GA:TMC)			
Wafer	56.6	18.5	24.9	3.9	1.1	1.5	Wafer	57.3	18.2	24.5	4.1	1.1	1.5
Wafer-RSP	56.6	18.5	24.9	3.9	1.1	1.5	Wafer-RSP	57.3	18.2	24.5	4.1	1.1	1.5
Rod	57.4	17.6	25.0	3.9	1.1	1.5	Rod	57.3	18.2	24.5	4.0	1.1	1.5
Rod-RSP	57.1	17.5	25.4	3.9	1.1	1.5	Rod-RSP	58.0	17.9	24.10	4.10	1.1	1.5
			P(D,L-LA:GA:CL)							P(L-LA:GA:CL)			
Wafer	70.5	13.4	16.1	10.3	1.8	1.2	Wafer	70.3	12.6	17.1	9.2	1.4	1.2
Wafer-RSP	70.7	13.4	16.0	10.3	1.8	1.2	Wafer-RSP	70.3	12.6	17.1	9.1	1.4	1.2
Rod	70.6	13.4	16.0	10.3	1.7	1.2	Rod	71.5	12.3	16.2	9.51	1.4	1.2
Rod-RSP	71.1	13.0	15.9	10.3	1.8	1.2	Rod-RSP	71.3	12.4	16.3	8.8	1.4	1.2

F_{LL} – molar percentage of lactidyl units in terpolymer.
F_{GG} – molar percentage of glycolidyl units in terpolymer.
F_{TMC} – molar percentage of carbonate units in terpolymer.
F_{CL} – molar percentage of caproyl units in terpolymer.
l_{LL} – average length of lactidyl blocks.
l_{GG} – average length of glycolidyl blocks.
l_{TMC} – average length of carbonate blocks.
l_{CL} – average length of caproyl blocks.

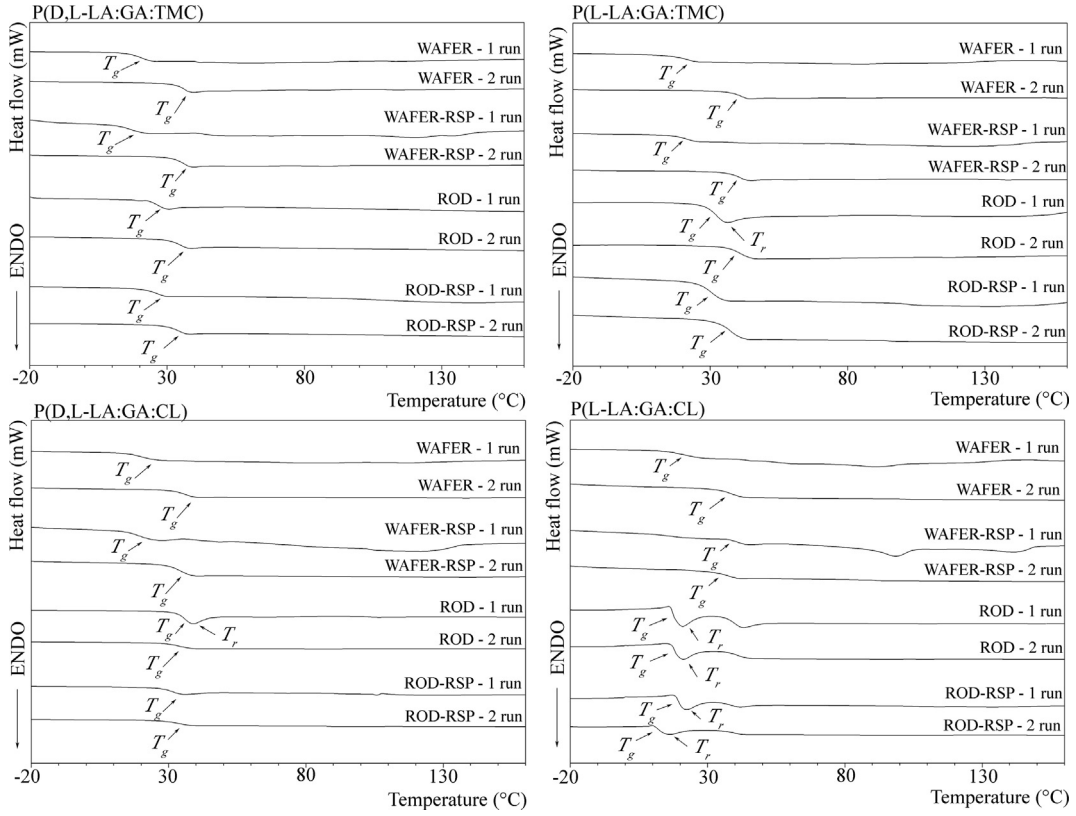

Fig. 8. DSC curves of the first and second heating runs for wafers, wafers-RSP, rods, and rods-RSP formulated from P(D,L-LA:GA:TMC), P(L-LA:GA:TMC), P(D,L-LA:GA:CL), and P(L-LA:GA:CL).

4.2. Thermal properties of terpolymers

DSC measurement of P(D,L-LA:GA:TMC), P(L-LA:GA:TMC), P(D,L-LA:CL), and P(L-LA:GA:CL) revealed a lack of melting endotherms, which proved the drug carriers' amorphous character (Table 3). This points to the possibility of composite formation between the crystalline drug substance (RSP) and the amorphous terpolymers. The same effect was previously observed for sirolimus and P(D,L-LA:GA:TMC) (Jaworska et al., 2015), and for estradiol and P(L-LA:GA:TMC) (Turek et al., 2016). The processing temperature for the amorphous polymer should be determined from T_g, as opposed to semi-crystalline polymers, for which T_m is applied.

In this study, the formulation conditions for HME should have been selected on the basis of T_g, i.e., above 33.8–39.8 °C (Table 3). However, ensuring flow behavior for the extruded material was also significant. Here, the terpolymers possessed thermoplastic properties. Flow temperature was empirically determined at a level of 105 °C, which is also safe for RSP, as each processing temperature should not exceed 171 °C. The thermal conditions had lesser meaning in SC because the formulation process was carried out at 25 °C.

T_g is also important in the design of polymer drug delivery systems for prolonged release. According to the literature, T_g of the applied

Table 5
Parameters characterizing wafers, wafers-RSP, rods, and rods-RSP formulated from P(D,L-LA:GA:TMC), P(L-LA:GA:TMC), P(D,L-LA:GA:CL), and P(L-LA:GA:CL).

Sample	T_r	T_g	M_n	D	Sample	T_r	T_g	M_n	D
		P(D,L-LA:GA:TMC)					P(L-LA:GA:TMC)		
Wafer	ND	35.0	39.9	2.081	Wafer	ND	39.8	45.4	1.953
Wafer-RSP	ND	35.0	29.2	2.154	Wafer-RSP	ND	39.4	41.1	1.910
Rod	ND	34.0	29.1	2.412	Rod	38.2	40.4	44.6	2.048
Rod-RSP	ND	33.00	13.3	2.905	Rod-RSP	ND	40.0	23.7	2.402
		P(D,L-LA:GA:CL)					P(L-LA:GA:CL)		
Wafer	ND	33.8	66.9	2.334	Wafer	ND	38.2	39.0	2.108
Wafer-RSP	ND	33.7	59.9	2.289	Wafer-RSP	ND	38.1	34.6	2.023
Rod	39.00	33.6	48.1	2.438	Rod	43.2	40.8	39.6	2.923
Rod-RSP	ND	32.5	26.8	2.691	Rod-RSP	42.2	39.5	27.3	2.249

T_r – temperature of structural relaxation (°C).
T_g – glass transition temperature (°C).
M_n – molecular weight (kDa).
D – molecular weight distribution.
ND – non-detected.

polymers is higher than body temperature in most formulations. According to data in the literature, for formulations with RSP, polymers have T_g in the range of 40 °C to 60 °C (Acharya et al., 2010; An et al., 2016; D'Souza et al., 2014a; Navitha et al., 2014; Panda et al., 2016; Rawat et al., 2011; Rawat et al., 2012; Selmin et al., 2012; Shen et al., 2015; Shen et al., 2016, Turek et al., 2015; Wang et al., 2002). Drug carriers exposed to temperatures above T_g will exhibit an increase in free volume, which will permit greater local segmental chain mobility and faster drug release.

It was revealed that T_g was above body temperature for P(L-LA:GA:TMC) and P(L-LA:GA:CL) and lower for P(D,L-LA:GA:TMC) and P(D,L-GA:LA:CL) (Table 3), which was reflected in the release profiles. Formulations with T_g in the range of 38.1 °C to 40.8 °C revealed a release period from 85 days to 127 days, whereas formulations with T_g from 32.5 °C to 35 °C released RSP from 75 days to 99 days (Table 5; Fig. 11). Moreover, polymers with lower T_g can be useful for the formulation of delivery systems based on blends, as they may allow to deliver the initial dose (bolus) in the first phase of release and then prolonged release during the whole process of degradation. They can thus be used in order to decrease the release period, which was revealed for P(L-LA:GA:CL).

The formulation method should not significantly influence T_g due to

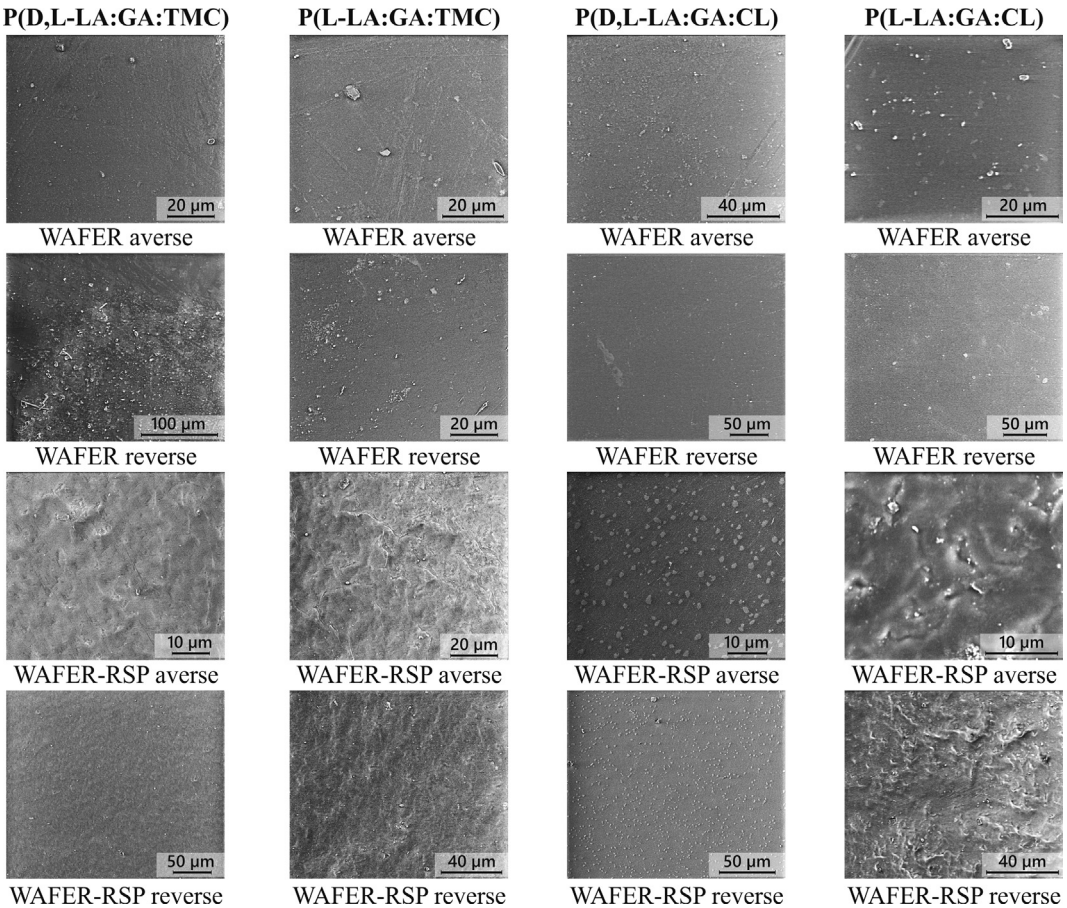

Fig. 9. SEM images of the P(D,L-LA:GA:TMC) wafer, P(D,L-LA:GA:TMC) wafer-RSP, P(L-LA:GA:TMC) wafer, P(L-LA:GA:TMC) wafer-RSP, P(D,L-LA:GA:CL) wafer, P(D,L-LA:GA:CL) wafer-RSP, P(L-LA:GA:CL) wafer, and P(L-LA:GA:CL) wafer-RSP.

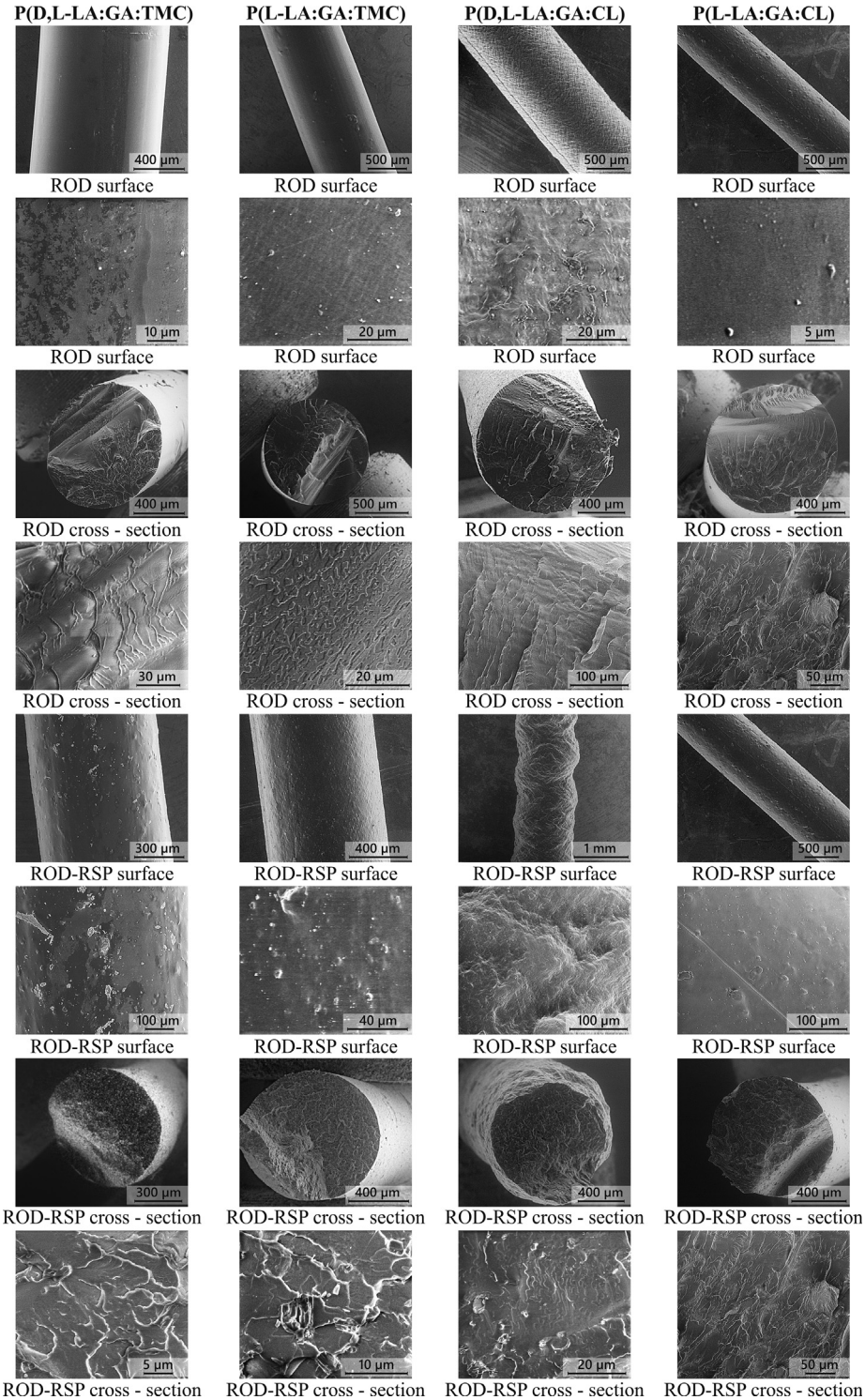

Fig. 10. SEM images of the P(D,L-LA:GA:TMC) rod, P(D,L-LA:GA:TMC) rod-RSP, P(L-LA:GA:TMC) rod; P(L-LA:GA:TMC) rod-RSP, P(D,L-LA:GA:CL) rod, P(D,L-LA:GA:CL) rod-RSP, P(L-LA:GA:CL) rod, and P(L-LA:GA:CL) rod-RSP.

the risk of bioavailability changes. SC and HME as used in this study did not change this parameter (Table 5). It should also be noted that the solvent and drug substances may act as either plasticizers or anti-plasticizers, i.e., T_g either decreases or increases. However, these effects were not noted in this study. This may show that our samples did not contain significant amounts of water (moisture) and other solvents (Santoveña et al., 2005; Snejdrova et al., 2013, 2016).

Another interesting phenomenon was observed in this study. In the analyzed samples, an endothermal event following T_g was revealed for P(L-LA:GA:TMC), P(D,L-LA:GA:CL), and P(L-LA:GA:CL) rods, and for P(L-LA:GA:CL) rods-RSP (Fig. 8, Table 5). This effect reflects the enthalpy of structural relaxation, which depends on the storage and processing temperature. It should be noted that amorphous glassy polymers are thermodynamically unstable and their structure relaxes toward the equilibrium state after processing. Data in the literature point to the fact that relaxation events are revealed in the region of T_g (Armeniades and Baer, 1977; Badii et al., 2005; Berens and Hodge, 1982, Chung and Lim, 2003a,b, 2004; Hung et al., 2002). It should also

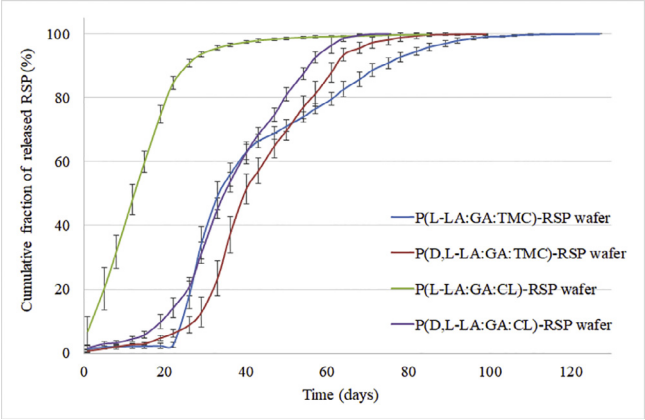

Fig. 11. Cumulative release profile of RSP from wafers-RSP and rods-RSP.

be noted that T_g and structural relaxation are two major transitions in amorphous polymers.

In this study, rods were obtained by HME. This process is based on compressing materials under high pressure which are then forced to pass through a die of an adequate shape. The observed endotherms can result from the orientation of the terpolymer fibers during HME. Re-ordering of the fibers took place during the first heating run. On the other hand, the additional endotherm may have resulted from incomplete amorphization of CL.

Relaxation may also result from the DSC measurements. It has been confirmed that enthalpy relaxation may occur when the cooling rate is slower than the heating rate. In our study, we used quenching as a cooling procedure to obtain amorphous samples which was faster than the heating rate (20 °C/min).

4.3. Terpolymer composition and chain microstructure

The polymer's composition and chain microstructure are important features that decide about the degradation rate and release pattern. For PLGA copolymers, a higher content of GA accelerated the release process (Acharya et al., 2010; An et al., 2016; D'Souza et al., 2013, 2014a,b; Hu et al., 2011; Jafarifar et al., 2016; Jaworska et al., 2015; Mittal et al., 2007; Park, 1996; Selmin et al., 2012; Shen et al., 2016; Song et al., 2014; Su et al., 2009; Tian et al., 2014; Turek et al., 2015, 2016; Wang et al., 2002; Zilberman and Grinber, 2008). Tailoring and determining these parameters is significant at the stage of design, as various components have been proposed to optimize the features of drug delivery systems, e.g., LA, GA, TMC, and CL (D'Souza et al., 2014a,b; Megens et al., 1988; Mittal et al., 2007; Park, 1996; Turek et al., 2015, 2016; Zilberman and Grinber, 2008). These components possess different thermal stability, which may play a key role during the formulation process at higher temperatures.

In this study, the average length of the blocks was determined for the chain microstructure. No significant changes took place in the terpolymers' chain microstructure during the formulation process. Both SC and HME allowed to retain the initial terpolymers' composition and chain microstructure in formulations with and without RSP. The application of P(L-LA:GA:CL) resulted in a two-phase release pattern, and a three-phase pattern was revealed for the other terpolymers (Fig. 11).

4.4. Molecular weight

M_n is one of the important parameters in the design of drug carriers based on aliphatic polyesters. M_n is closely related to drug release, polymer degradation, and storage (Turek et al., 2015, 2016). D'Souza and co-workers showed that PLGA copolymers with M_n of 15 kDa and 30 kDa revealed faster release of olanzapine-loaded microspheres and the degradation process than copolymers with higher M_n (82 kDa and 131 kDa) (D'Souza et al., 2014a). In our previous study we also pointed to significant differences in the degradation period between L-PLGA 85:15 (100 kDa) and P(L-LA:GA:TMC) with a ratio of 57:19:24 (59 kDa). Lower values influence faster degradation of drug carriers (Turek et al., 2015, 2016). For this reason, a study regarding the influence of the formulation process on the M_n value was significant for pharmaceutical manufacture since the value of M_n may decrease significantly as a result of the formulation process.

In this study, some findings were noted in the context of M_n and the formulation process, namely (i) M_n decreased after SC, (ii) HME resulted in a drop in M_n to a greater extent than SC, and (iii) the introduction of RSP into the wafer and rods influenced further decreases in M_n (Table 5).

These issues have been presented in data in the literature. Microparticle formulation via the encapsulation method requires significant amounts of the solvent. Selmin and co-workers (2012) showed that manufacturing blank microspheres from D,L-PLGA 65:35 and D,L-PLGA 85:15 by the extraction/evaporation method in an aqueous environment resulted in a decrease in M_n by ca. 4% and 5%, respectively, in comparison to raw polymers. It may thus be suggested that only dissolution of aliphatic polyesters results in an M_n decrease. Moreover, the introduction of RSP resulted in a drop in M_n by 20% and 10%, respectively, in comparison to raw polymers. The researchers explained that the reason for this effect lay in the use of RSP in solution (Selmin et al., 2012).

In this study, for wafers and wafers-RPS, the SC method influenced a decrease in M_n between 12–26% and 21–41%, respectively. It should be noted that small amounts of methylene chloride were used in SC. The decrease in M_n may have resulted from the presence of water in the solvent. It is understandable that more solvent was used for the formulation of wafers-RSP, which reflected a higher decrease in M_n.

One of the features of aliphatic polyesters is their thermoplasticity, therefore melt-processing is adequate for drug formulation. However, melt-processing is often problematic due to thermal and hydrolytic instability (Ellä et al., 2011).

A decrease in M_n for HME was also observed. A study on thermal degradation during melt-processing performed by other researchers revealed a decrease in M_n between 27% and 69% (Cicero and Dorgan, 2001; Gogolewski et al., 1993; Nuutinen et al., 2002; Rothen-Weinhold et al., 1997; Rothen-Weinhold et al., 1999; Simpson et al., 2015; Yen et al., 2009; Yuan et al., 2001).

Our results reflected the above results, as an M_n decrease for rods and rods-RSP was observed (Table 5). According to data in the literature, this phenomenon may have been caused by the presence of moisture and oxygen. In theory, moisture can be eliminated by drying, whereas the impact of atmospheric oxygen can be minimized by using an inert gas (Ellä et al., 2011). In practice, the total elimination of both water and oxygen during formulation is practically impossible. Ella and co-workers also showed that sufficient drying did not eliminate the drop in M_n that was noted at a level of 47–64%, therefore, the researchers suspected that other factors also played a significant role in the M_n drop, i.e., the formulation temperature and time residence in the extruder, and the shear stress exerted on the polymer (Ellä et al., 2011). According to Liu et al., degradation during processing may be caused by random chain scission. Additionally, acidic degradation products enhance the autocatalytic degradation process, which leads to a subsequent drop in M_n (Liu et al., 2006).

In our study, the lowest value of M_n was 13.3 kDa for P(D,L-LA:GA:TMC) RSP-rods (Table 5), however, this material can be considered useful, which was confirmed by the release profile (Fig. 11). It should be added that a polymer with low M_n may ensure zero-order release for estradiol. Mittal and co-workers indicated zero-order release of estradiol from PLGA nanoparticles with a M_n of 14.5 kDa and 45 kDa, whereas estradiol was released for PLGA nanoparticles with a M_n of 85 kDa and 213 kDa according to Higuchi's pattern (Mittal et al., 2007). Our previous study also pointed to a zero-order release pattern for P(L-

LA:GA:TMC) with a M_n of 59 kDa (Turek et al, 2016). This fact was not observed for RSP in this study (Fig. 11).

The influence of M_n (Table 5) on the release period is shown for the formulation with a terpolymer with racemic and optically active LA, GA, and TMC (Fig. 11). For the P(L-LA:GA:TMC) wafers-RSP (41.1 kDa) and P(L-LA:GA:TMC) rods-RSP (23.7 kDa), the release period was longer than for P(D,L-LA:GA:TMC) wafers-RSP (29.2 kDa) and P(D,L-LA:GA:TMC) rods-RSP (13.3 kDa). This rule was not observed in the case of terpolymers with CL (Table 5, Fig. 3), although it should be emphasized that the release process is the resultant of many variables.

Therefore, the formulation obtained by SC and HME may offer interesting solutions for RSP delivery; however, the M_n decrease should be considered when designing new drug formulations.

4.5. Morphology

The important role of surface and inner structure of the drug formulation is known in the literature (Fredenberg et al., 2011; Turek et al., 2015, 2016), and which the results of this study also confirmed. None of the formulations showed pores, cracks, or slits on the surfaces (Figs. 9 and 10), which minimalized an uncontrolled burst in the obtained release profiles (Fig. 11) (Janoria and Mitra, 2007). The greatest morphological diversity was observed for the averse of P(L-LA:GA:CL) wafers-RSP (Fig. 9), which may have influenced the presence of the burst effect (Fig. 11).

4.6. Release process of RSP

RSP was released in three phases, however, the burst effect was revealed for P(L-LA:GA:CL) wafers-RSP and rods-RSP. Generally, these release patterns are most often exhibited for PLGA copolymers, which the data in the literature also confirm for RSP release (D'Souza et al., 2013, Navitha et al., 2014; Rawat et al., 2012; Selmin et al., 2012).

The release pattern is related to both the shape and the size of the formulations. Generally, according to Sansdrap and Moës (1997) and Fredenberg et al. (2011), for PLGA copolymers the bi-phasic model is characteristic of small particles and thin films. Berchane et al. (2007) and Berkland et al. (2003) pointed out that tri-phasic release takes place due to heterogeneous degradation of large particles. However, drug substances are mainly released in the classic tri-phasic profile from PLGA copolymers. The first phase is usually determined as a burst effect and is attributed to non-entrapped substance molecules in the polymer structure. The burst effect may also be attributed to drug molecules close to the surface that are easily accessible by hydration (Wang et al., 2002). Thus burst release is determined as a stage of the release mechanism and as a surface phenomenon with neither a negative nor a positive role, i.e., the burst effect has no strict definition. Yet according to some authors the burst effect is assigned negative occurrences, i.e., cracks and disintegration (Huang and Brazel, 2001; Janoria and Mitra, 2007). Uncontrolled release may influence a decrease in the total drug dose tailored for the formulation with prolonged release. Phases II and III are often called the slow-release phase (slow drug diffusion) and the fast-release phase (erosion onset), respectively. This tri-phasic profile was observed for all of the obtained formulations that are characteristic of large particles (Berchane et al. 2007; Berkland et al., 2003).

The burst effect was noted for P(L-LA:GA:CL) wafers-RSP and rods-RSP. We believe that these release patterns did not represent the bi-phasic model since overlap of the first and second phases took place. It should be noted that the greatest morphological diversity was observed for the averse of P(L-LA:GA:CL) wafers-RSP, which may be related to the presence of RSP molecules close to the surface (Fig. 9).

Generally, the wafers' release period was similar to that for the rods, except for P(L-LA:GA:CL) wafers-RSP, for which it was shorter. Terpolymers with optically active LA showed a longer release period in comparison to terpolymers with racemic LA (Fig. 11), which also resulted from the properties of the applied raw terpolymers and formulations (Figs. 2–11, Tables 3–5). It is difficult to state which feature was dominant for the release process, nevertheless the obtained formulations may be an interesting therapeutic solution in prolonging administration intervals and the release period in comparison to the commercial product.

5. Conclusions

The study presented here points to the following: (i) the thermal properties of RSP and the applied terpolymers enable processing by SC and HME; (ii) SC resulted in a lower decrease in M_n than HME, and the introduction of RSP to the terpolymers influenced another drop in this parameter; (iii) no changes in the other parameters were observed as a result of the formulation process; (iv) the release process underwent three phases and (v) none of the applied terpolymers revealed significant benefits when compared to one another at this stage of the study in the formulation process.

Reassuming, SC and HME are adequate methods for the formulation of biodegradable drug delivery systems (wafers and rods, respectively) based on the proposed terpolymers.

Acknowledgments

This work was financially supported by the National Centre for Research and Development, RYSPCONT [Grant Number PBS1/A7/2/2012].

References

Acharya, G., Shin, C.S., Vedantham, K., McDermott, M., Rish, T., Hansen, K., Fu, Y., Park, K., 2010. A study of drug release from homogeneous PLGA microstructures. J. Control. Release 146, 201–206.
An, T., Choi, J., Kim, A., Lee, J.H., Nam, Y., Park, J., Sun, B.K., Suh, H., Kim, C.J., Hwang, S.J., 2016. Sustained release of risperidone from biodegradable microspheres prepared by in-situ suspension-evaporation process. Int. J. Pharm. 503, 8–15.
Armeniades, C.D., Baer, E., 1977. Transitions and relaxations in polymers. In: Kaufman, H.S., Falcetta, J.J. (Eds.), Introduction to Polymer Science and Technology. Wiley and Sons, New York, pp. 239–301.
Badii, F., MacNaughtan, W., Farhat, I., 2005. Enthalpy relaxation of gelatin in the glassy state. Int. J. Biol. Macromol. 36, 263–269.
Berchane, N.S., Carson, K.H., Rice-Ficht, A.C., Andrews, M.J., 2007. Effect of mean diameter and polydispersity of PLG microspheres on drug release: experiment and theory. Int. J. Pharm. 337, 118–126.
Berens, A.R., Hodge, I.M., 1982. Effects of annealing and prior history on enthalpy relaxation in glassy polymers. 1. Experimental study on poly(vinyl chloride). Macromolecules 15, 756–761.
Borison, R.L., Pathiraja, A.P., Diamond, B.I., Meibach, R.C., 1992. Risperidone: clinical safety and efficacy in schizophrenia. Psychopharmacol. Bull. 28, 213–218.
Chen, W., Meng, F., Cheng, R., Deng, C., Feijen, J., Zhong, Z., 2014. Advanced drug and gene delivery systems based on functional biodegradable polycarbonates and copolymers. J. Control. Release 190, 398–414.
Chung, H.J., Lim, S.T., 2003a. Physical aging of glassy normal and waxy rice starches: effect of aging time on glass transition and enthalpy relaxation. Food Hydrocolloids 17, 855–861.
Chung, H.J., Lim, S.T., 2003b. Physical aging of glassy normal and waxy rice starches: effect of aging temperature on glass transition and enthalpy relaxation. Carbohyd. Polym. 53, 205–211.
Chung, H.J., Lim, S.T., 2004. Physical aging of glassy normal and waxy rice starches: thermal and mechanical characterization. Carbohyd. Polym. 57, 15–21.
Cicero, J.A., Dorgan, J.R., 2001. Physical properties and fiber morphology of poly(lactic acid) obtained from continuous two-steps melt spinning. J. Polym. Environ. 9, 1–10.
Czajkowska, B., Dobrzynski, P., Bero, M., 2005. Interaction of cells with L-lactide/glycolide copolymers synthesized with the use of tin or zirconium compounds. J. Biomed. Mater. Res. A 74, 591–597.
Dobrzynski P., Kasperczyk J., Smola A., Pastusiak M., Sobota M., 2013. Bioresorbable and biocompatible thermoplastic elastomer having a shape memory, particularly for biomedical applications and a process for their preparation. EP 2647656 A2.
D'Souza, S., Faraj, J., DeLuca, P., 2013. Microsphere delivery of risperidone as an alternative to combination therapy. Eur. J. Pharm. Biopharm. 85, 631–639.
D'Souza, S., Faraj, J.A., Giovagnoli, S., Deluca, P.P., 2014a. IVIVC from long acting olanzapine microspheres. Int. J. Biomater. 2014, 407065.
D'Souza, S., Faraj, J.A., Giovagnoli, S., Deluca, P.P., 2014b. Development of Risperidone PLGA Microspheres. J. Drug. Deliv. 2014, 620464.
Ellä, V., Nikkola, L., Kellomäki, M., 2011. Process-induced monomer on a medical-grade polymer and its effect on short-term hydrolytic degradation. J. Appl. Polym. Sci. 119, 2996–3003.
Fleischhacker, W.W., Eerdekens, M., Karcher, K., Remington, G., Llorca, P.M.,

Chrzanowski, W., Martin, S., Gefvert, O., 2003. Treatment of schizophrenia with long-acting injectable risperidone: a 12-month open-label trial of the first long-acting second-generation antipsychotic. J. Clin. Psychiatry 10, 1250–1257.
Fredenberg, S., Wahlgren, M., Reslow, M., Axelsson, A., 2011. The mechanisms of drug release in poly(lactic-co-glycolic acid)-based drug delivery systems–a review. Int. J. Pharm. 415, 34–52.
Gebarowska, K., Kasperczyk, J., Dobrzynski, P., Scandola, M., Zini, E., Li, S., 2011. NMR analysis of the chain microstructure of biodegradable terpolymers with shape memory properties. Eur. Polym. J. 47, 1315–1327.
Gogolewski, S., Jovanovic, M., Perren, S.M., Dillon, J.G., Hughes, M.K., 1993. The effect of melt-processing on the degradation of selected polyhydroxyacids: polylactides, polyhydroxybutyrate, and polyhydroxybutyrate-co-valerates. Polym. Degrad. Stabil. 40, 313–322.
Harrison, T.S., Goa, K.L., 2004. Long-acting risperidone: a review of its use in schizophrenia. CNS Drugs 18, 113–132.
Hillert, A., Maier, W., Wetzel, H., Benkert, O., 1992. Risperidone in the treatment of disorders with a combined psychotic and depressive syndrome–a functional approach. Pharmacopsychiatry 25, 213–217.
http://www.ema.europa.eu/docs/en_GB/document_library/Referrals_document/Risperdal_Consta_30/WC500008170.pdf (Accessed 8 Jan 2017).
Hu, Z., Liu, Y., Yuan, W., Wu, F., Su, J., Jin, T., 2011. Effect of bases with different solubility on the release behavior of risperidone loaded PLGA microspheres. Colloids Surf., B 86, 206–211.
Huang, X., Brazel, C.S., 2001. On the importance and mechanisms of burst release in matrix-controlled drug delivery systems. J. Control. Release 73, 121–136.
Hung, H.J., Lee, E.J., Lim, S.T., 2002. Comparison in glass transition and enthalpy relaxation between native and gelatinized rice starches. Carbohyd. Polym. 28, 287–298.
Jafarifar, E., Hajialyani, M., Akbari, M., Rahimi, M., Shokoohinia, Y., Fattahi, A., 2016. Preparation of a reproducible long-acting formulation of risperidone-loaded PLGA microspheres using microfluidic method. Pharm. Dev. Technol. 8, 1–8.
Janoria, K.G., Mitra, A.K., 2007. Effect of lactide/glycolide ratio on the in vitro release of ganciclovir and its lipophilic prodrug (GCV-monobutyrate) from PLGA microspheres. Int. J. Pharm. 338, 133–141.
Janssen, P.A., Niemegeers, C.J., Awouters, F., Schellekens, K.H., Megens, A.A., Meert, T.F., 1988. Pharmacology of risperidone (R 64 766), a new antipsychotic with serotonin-S2 and dopamine-D2 antagonistic properties. J. Pharmacol. Exp. Ther. 244, 685–693.
Jaworska, J., Jelonek, K., Sobota, M., Kasperczyk, J., Dobrzynski, P., Musial-Kulik, M., Smola-Dmochowska, A., Janeczek, H., Jarzabek, B., 2015. Shape-memory bioresorbable terpolymer composite with antirestenotic drug. J. Appl. Polym. Sci. 132, 41902.
Jelonek, K., Kasperczyk, J., Li, S., Dobrzynski, P., Jarzabek, B., 2011. Controlled poly(l-lactide-co-trimethylene carbonate) delivery system of cyclosporine A and rapamycine–the effect of copolymer chain microstructure on drug release rate. Int. J. Pharm. 414, 203–209.
Kasperczyk, J., Stoklosa, K., Dobrzynski, P., Stepien, K., Kaczmarczyk, B., Dzierzega-Lecznar, A., 2009. Designing bioresorbable polyester matrices for controlled doxorubicin release in glioma therapy. Int. J. Pharm. 382, 124–129.
Li, D., Guo, G., Deng, X., Fan, R., Guo, Q., Fan, M., Liang, J., Luo, F., Qian, Z., 2013a. PLA/PEG-PPG-PEG/dexamethasone implant prepared by hot-melt extrusion for controlled release of immunosuppressive drug to implantable medical devices, Part 2: in vivo evaluation. Drug Deliv. 20, 134–142.
Li, D., Guo, G., Fan, R., Liang, J., Deng, X., Luo, F., Qian, Z., 2013b. PLA/F68/dexamethasone implants prepared by hot-melt extrusion for controlled release of anti-inflammatory drug to implantable medical devices: I. Preparation, characterization and hydrolytic degradation study. Int. J. Pharm. 441, 365–372.
Liu, X., Zou, Y., Li, W., Cao, G., Chen, W., 2006. Kinetics of thermo-oxidative and thermal degradation of poly(D, L–lactide) (PDLLDA) at processing temperature. Polym. Degrad. Stab. 91, 3259–3265.
Lu, Y., Sturek, M., Park, K., 2014. Microparticles produced by the hydrogel template method for sustained drug delivery. Int. J. Pharm. 461, 258–269.
Ma, D., McHugh, A.J., 2010. The interplay of membrane formation and drug release in solution-cast films of polylactide polymers. Int. J Pharm. 388, 1–12.
Manson, J., Dixon, D., 2012. The influence of solvent processing on polyester bioabsorbable polymers. J. Biomater. Appl. 26, 623–634.
Martin, S.D., Libretto, S.E., Pratt, D.J., Brewin, J.S., Huq, Z.U., Saleh, B.T., 2003. Clinical experience with the long-acting injectable formulation of the atypical antipsychotic, risperidone. Curr. Med. Res. Opin. 19, 298–305.
Megens, A.A., Awouters, F.H., Niemegeers, C.J., 1988. Differential effects of the new antipsychotic risperidone on large and small motor movements in rats: a comparison with haloperidol. Psychopharmacology (Berl) 95, 493–496.
Mittal, G., Sahana, D.K., Bhardwaj, V., Ravi Kumar, M.N., 2007. Estradiol loaded PLGA nanoparticles for oral administration: effect of polymer molecular weight and copolymer composition on release behaviour in vitro an in vivo. J. Control. Release 119, 77–85.
Navitha, A., Jogala, S., Krishnamohan, C., Aukunuru, J., 2014. Development of novel risperidone implants using blends of polycaprolactones and in vitro in vivo correlation studies. J. Adv. Pharm. Technol. Res. 5, 84–89.
Nuutinen, J.P., Clerc, C., Virta, T., Törmälä, P., 2002. Effect of gamma, ethylene oxide, electron beam, and plasma sterilization on the behaviour of SR-PLLA fibres in vitro. J. Biomater. Sci. Polym. Ed. 13, 1325–1336.
Orchel, A., Jelonek, K., Kasperczyk, J., Dobrzynski, P., Marcinkowski, A., Pamula, E., Orchel, J., Bielecki, I., Kulczycka, A., 2013. The influence of chain microstructure of biodegradable copolyesters obtained with low-toxic zirconium initiator to in vitro biocompatibility. Biomed. Res Int. 2013, 176946.
Panda, A., Meena, J., Katara, R., Majumdar, D.K., 2016. Formulation and characterization of clozapine and risperidone co-entrapped spray-dried PLGA nanoparticles. Pharm. Dev. Technol. 21, 43–53.
Park, T.G., 1996. Degradation of poly(lactic-co-glycolic acid) microspheres: effect of copolymer composition. Biomaterials 16, 1123–1130.
Rahman, Z., Zidan, A.S., Khan, M.A., 2010a. Non-destructive methods of characterization of risperidone solid lipid nanoparticles. Eur. J. Pharm. Biopharm. 76, 127–137.
Rahman, Z., Zidan, A.S., Khan, M.A., 2010b. Risperidone solid dispersion for orally disintegrating tablet: its formulation design and non-destructive methods of evaluation. Int. J. Pharm. 400, 49–58.
Rattanakit, P., Moulton, S.E., Santiago, K.S., Liawruangrath, S., Wallace, G.G., 2012. Extrusion printed polymer structures: a facile and versatile approach to tailored drug delivery platforms. Int. J. Pharm. 422, 254–263.
Rawat, A., Bhardwaj, U., Burgess, D.J., 2012. Comparison of in vitro-in vivo release of Risperdal(®) Consta(®) microspheres. Int. J. Pharm. 434, 115–121.
Rawat, A., Stippler, E., Shah, V.P., Burgess, D.J., 2011. Validation of USP apparatus 4 method for microsphere in vitro release testing using Risperdal Consta. Int. J. Pharm. 420, 198–205.
Ro, A.J., Falotico, R., Davé, V., 2012. Morphological and degradation studies of sirolimus-containing poly(lactide-co-glycolide) discs. J. Biomed. Mater. Res. B 100, 767–777.
Rothen-Weinhold, A., Besseghir, K., Gurny, R., 1997. Analysis of the influence of polymer characteristics and core loading on the in vivo release of a somatostatin analogue. Eur. J. Pharm. Sci. 5, 303–313.
Rothen-Weinhold, A., Besseghir, K., Vuaridel, E., Sublet, E., Oudry, N., Kubel, F., Gurny, R., 1999. Injection-molding versus extrusion as manufacturing technique for the preparation of biodegradable implants. Eur. J. Pharm. Biopharm. 48, 113–121.
Rychter, P., Pamula, E., Orchel, A., Posadowska, U., Krok-Borkowicz, M., Kaps, A., Smigiel-Gac, N., Smola, A., Kasperczyk, J., Prochwicz, W., Dobrzynski, P., 2015. Scaffolds with shape memory behavior for the treatment of large bone defects. J. Biomed. Mater. Res. A. 103, 3503–3515.
Sansdrap, P., Moës, A.J., 1997. In vitro evaluation of the hydrolytic degradation of dispersed and aggregated poly(ɒ;-lactide-co-glycolide) microspheres. J. Control. Release. 43, 47–58.
Santoveña, A., Alvarez-Lorenzo, C., Concheiro, A., Llabrés, M., Fariña, J.B., 2005. Structural properties of biodegradable polyesters and rheological behavior of their dispersions and films. J. Biomater. Sci. Polym. Ed. 16, 629–641.
Selmin, F., Blasi, P., DeLuca, P.P., 2012. Accelerated polymer biodegradation of risperidone poly(D, L-lactide-co-glycolide) microspheres. AAPS Pharm. Sci. Tech 13, 1465–1472.
Shen, J., Choi, S., Qu, W., Wang, Y., Burgess, D.J., 2015. In vitro-in vivo correlation of parenteral risperidone polymeric microspheres. J. Control. Release 218, 2–12.
Shen, J., Lee, K., Choi, S., Qu, W., Wang, Y., Burgess, D.J., 2016. A reproducible accelerated in vitro release testing method for PLGA microspheres. Int. J. Pharm. 498, 274–282.
Simpson, R.L., Nazhat, S.N., Blaker, J.J., Bismarck, A., Hill, R., Boccaccini, A.R., Hansen, U.N., Amis, A.A., 2015. A comparative study of the effects of different bioactive fillers in PLGA matrix composites and their suitability as bone substitute materials: A thermo-mechanical and in vitro investigation. J. Mech. Behav. Biomed. Mater. 50, 277–289.
Snejdrova, E., Dittrich, M., Drastik, M., 2013. Plasticized branched aliphatic oligoesters as potential mucoadhesive drug carriers. Int. J. Pharm. 458, 282–286.
Snejdrova, E., Drastik, M., Dittrich, M., Kastner, P., Nguyenova, J., 2016. Mucoadhesive plasticized system of branched poly(lactic-co-glycolic acid) with aciclovir. Drug. Dev. Ind. Pharm. 42, 1653–1659.
Song, G.M., Kim, H.Y., Ryu, J.H., Chu, C.W., Kang, D.H., Park, S.B., Jeong, Y.I., 2014. Self-assembled polymeric micelles based on hyaluronic acid-g-poly(D, L-lactide-co-glycolide) copolymer for tumor targeting. Int. J. Mol. Sci. 15, 16057–16068.
Su, Z., Sun, F., Shi, Y., Jiang, C., Meng, Q., Teng, L., Li, Y., 2009. Effects of formulation parameters on encapsulation efficiency and release behavior of risperidone poly(D, L-lactide-co-glycolide) microsphere. Chem. Pharm. Bull. 57, 1251–1256.
Tian, J., Wang, W., Ye, L., Cen, X., Guan, X., Zhang, J., Yu, P., Du, G., Liu, W., Li, Y., 2014. A 12-week intramuscular toxicity study of risperidone-loaded microspheres in Beagle dogs. Hum. Exp. Toxicol. 33, 473–487.
Turek, A., Jelonek, K., Wójcik, A., Dzierżewicz, Z., Kasperczyk, J., Dobrzyński, P., Marcinkowski, A., Trzebicka, B., 2010. Surface properties of poly(L-lactide-co-glycolide) matrices with risperidone and their changes after two weeks of degradation. Eng. Biomater. 13, 117–120.
Turek, A., Kasperczyk, J., Jelonek, K., Borecka, A., Janeczek, H., Libera, M., Gruchlik, A., Dobrzyński, P., 2015. Thermal properties and morphology changes in degradation process of poly(L-lactide-co-glycolide) matrices with risperidone. Acta. Bioeng. Biomech. 17, 11–20.
Turek, A., Kasperczyk, J., Jelonek, K., Dobrzyński, P., Walichiewicz, J., Krzemińska, K., Smola, A., Musiał-Kulik, M., Marcinkowski, A., Libera, M., Gębarowska, K., Janeczek, H., 2013. Role of surface and structure in the initial release of risperidone from L-PLGA and D, L-PLGA matrices. Eng. Biomater. 16, 30–35.
Turek, A., Olakowska, E., Borecka, A., Janeczek, H., Sobota, M., Jaworska, J., Kaczmarczyk, B., Jarząbek, B., Gruchlik, A., Libera, M., Liśkiewicz, A., Jędrzejowska-Szypułka, H., Kasperczyk, J., 2016. Shape-memory terpolymer rods with 17-β-estradiol for the treatment of neurodegenerative diseases: an in vitro and in vivo study. Pharm. Res. 33, 2967–2978.
Wang, J., Wang, B.M., Schwendeman, S.P., 2002. Characterization of the initial burst release of a model peptide from poly(D, L-lactide-co-glycolide) microspheres. J. Control. Release 82, 289–307.
Weng, W., Quan, P., Liu, C., Zhao, H., Fang, L., 2016. Design of a drug-in-adhesive transdermal patch for risperidone: effect of drug-additive interactions on the crystallization inhibition and in vitro/in vivo correlation study. J. Pharm. Sci. 105,

3153–3161.
Wischke, C., Schwendeman, S.P., 2012. Degradable polymeric carriers for parenteral controlled drug delivery. In: Siepmann, J., Siegel, R.A., Rathbone, M.J. (Eds.), Fundamentals and Applications of Controlled Release Drug Delivery. Springer, New York, pp. 171–228.
Yen, H.J., Tseng, C.S., Hsu, S.H., Tsai, C.L., 2009. Evaluation of chondrocyte growth in the highly porous scaffolds made by fused deposition manufacturing (FDM) filled with type II collagen. Biomed. Microdevices 11, 615–624.
Yuan, X., Mak, A.F.T., Kwok, K.W., Yung, B.K.O., Yao, K., 2001. Characterization of poly (L-lactic acid) fibers produced by melt spinning. J. Appl. Polym. Sci. 81, 251–260.
Zilberman, M., Grinber, O., 2008. HRP-loaded biodegradable microspheres: effect of copolymer composition and molecular weight on microstructure and release profile. J. Biomater. Appl. 22, 391–407.
Zini, E., Scandola, M., Dobrzynski, P., Kasperczyk, J., Bero, M., 2007. Shape memory behavior of novel (L-lactide-glycolide-trimethylene carbonate) terpolymers. Biomacromolecules 8, 3661–3667.